Preprints of the 19th World Congress
The International Federation of Automatic Control
Cape Town, South Africa. August 24-29, 2014

Analytical Solution to the Minimum Energy Consumption Based Velocity Profile Optimization Problem With Variable Road Grade ⋆

Engin Ozatay * **Umit Ozguner** ** **John Michelini** *** **Dimitar Filev** ****

* *Electrical and Computer Engineering Department, The Ohio State University, Columbus OH 43210 USA (e-mail: ozatay.1@osu.edu).*
** *Electrical and Computer Engineering Department, The Ohio State University, Columbus OH 43210 USA (e-mail: ozguner.1@osu.edu).*
*** *Research and Innovation Center, Ford Motor Company, Dearborn, USA, (e-mail: jmichel1@ford.com)*
**** *Research and Innovation Center, Ford Motor Company, Dearborn, USA, (e-mail: dfilev@ford.com)*

Abstract: The importance of eco-driving in reducing cumulative fuel consumption of on road vehicles is a well known issue. However, so far a generic algorithm that can globally solve the non-linear optimization problem and still implementable in to the current state of computing on board units is not present. In this study, we examine one aspect of the problem by incorporating the effects of road grade to the optimization problem and generate an optimal velocity trajectory for a given road grade profile. We developed simple yet accurate vehicle and fuel consumption models and employed the models as the objective function and state trajectory constraint of the optimization problem. The necessary conditions derived by employing the calculus of variation theory require to separately solve the differential equations with a set of interior point constraints for each road grade interval. As the control became linear to the Hamiltonian function we defined a set of singular arcs and derived the state and optimal control input trajectories along the arcs. We have tested the analytical solution in two example problems and compared the results with a dynamic programming (DP) solution and constant speed cruise operation. The results have shown that the analytical and DP solutions generate very close velocity trajectories which are around $8-10\%$ more efficient than the constant cruise speed control case for the given examples. Moreover the calculation time of the analytical solution is significantly shorter than the DP solution rendering it possible to real-time on board implementations.

Keywords: Optimal control, intelligent cruise control, velocity control, variational analysis, vehicles, road grade

1. INTRODUCTION

In United States one third of global warming emissions adversely affecting human lives are due to transportation and more than 60% of the transportation emissions come from cars and light trucks, as reported by U.S. Transportation Department (2006). The situation is getting more severe as we consider the potential increase in the number of vehicles worldwide especially dominated by developing countries like China and India where the population is significantly high. As Dargay et al. (2007) reports in more developed countries like USA and Germany the number of vehicles per 100 people is almost saturated and the increase in number of vehicles is proportional to increase in population, however, in the developing countries there is a great potential in increase in number of vehicles as GDP per capita increases. Dargay et al. (2007) also reports that based on the historical data it is foreseen that in 2030 the number of vehicles on road will become 2 billions more than twice as it was in 2002 worldwide. Besides the effects of emissions on climate and human health, the studies in Owen et al. (2010) show that the oil resources are limited and will not be present for very long time. These limitations compel society, academia, and industry to seek efficient vehicles.

Many researchers have focused on velocity profile optimization referred as "Eco-Driving" as the area contains great potential in reducing cumulative fuel consumption of on road vehicles. The first work taking into account the variation in road grade was conducted by Schwarzkopf and Leipnik (1977), where the authors developed and solved a nonlinear optimal control problem by controlling the motor throttle to minimize the fuel consumption of the vehicle. Recently, Hellstrom et al. (2009) developed a look ahead control using dynamic programming (DP) to minimize fuel consumption considering change in road grade for trucks. Hellstrom et al. (2010) further extends the previous solution by formulating the problem using kinetic energy formulations of the vehicle and developed a more efficient DP algorithm. Chang and Morlok (2005) discusses the optimal steady state velocities of a vehicle under different road conditions including the effects of constant road grades.

The previous studies suggested either a complex closed form solution or sub optimal solutions or a numerical solution that

⋆ This paper is based on the work supported by Ford Motor Company, Deaborn, USA under the University Research Project (URP) Program.

is costly to be implemented to the existing on board computing units. In this study, we propose to extend the current state of the art of velocity profile optimization problem for minimum fuel consumption with varying road grade situations by developing fairly simple vehicle and fuel consumption models and solve the problem with very efficient analytic method such that it could be used for real-time on board computations.

2. MODELING

In this section we develop and present the longitudinal vehicle and fuel consumption models used in the optimization calculations.

2.1 Longitudinal Vehicle Model

In our previous work (Ozatay et al., 2013b) under the following conditions

- Vehicle operates at a constant gear,
- The model is linearized around an optimal constant velocity,
- Constant road grade,

we have developed a model of a vehicle's longitudinal velocity as

$$\dot{v} = \frac{1}{C_1(\gamma)}\left(C_2(\gamma)T_e - C_3^* v - C_4^*(\alpha) - F_{brake}\right), \qquad (1)$$

with the constants

$$C_1(\gamma) = \frac{1}{m_{eq}(\gamma)}, \quad C_2(\gamma) = \frac{\eta\gamma}{R_{wh}},$$
$$C_3 = \frac{1}{2}\rho A_f C_d, \quad C_4(\alpha) = mg\left(\cos(\alpha) r_0 + \sin(\alpha)\right),$$
$$C_3^* = 2C_3 v_{lin}, \qquad C_4^* = -C_3 v_{lin}^2 + C_4$$

where v is the longitudinal velocit, v_{lin} is the optimal constant velocity around which the equations are linearized, T_e is the engine torque, m_{eq} is the equivalent mass, m is the curb mass of the vehicle, F_{brake} is the brake force, α is the constant road grade, γ is the constant gear ratio, η is the transmission efficiency, R_{wh} is the radius of wheels, A_f is the frontal area, C_d is the drag coefficient, g is the gravitational force and r_0 is the friction constant of the tires.

In this work, we still employ (1) as the vehicle model, however, by considering the variations in $\alpha(t)$.

2.2 Fuel Consumption Model

As we aim to minimize the consumed fuel along a trip and solve the optimization problem analytically, we require a simple yet accurate fuel consumption model. The developed fuel consumption rate estimation model is based on the complex experimental model of the test vehicle Lincoln MKS 2008. The experimental fuel consumption model is defined by

$$\dot{m}_{f,exp} = P_3(\omega_e)\cdot T_e^3 + P_2(\omega_e)\cdot T_e^2 + P_1(\omega_e)\cdot T_e + P_0(\omega_e). \quad (2)$$

where ω_e is the engine speed. The experimentally obtained variables P_0, P_1, P_2, P_3 are reported in table 1.

Ozatay et al. (2013b) have designed a fuel consumption rate estimation model based on Willan's line approximation (Guzzella and Onder, 2010), however, we have observed that especially at high speed regions the model behaved poorly. In this work, we extend the model by increasing its degree of freedom with the addition of v^2 term. With the modification, we expect the model to compensate for the inaccuracies at high speed region. The equation of the developed fuel consumption rate estimation model is given by

Table 1. Fuel Consumption Model Parameter Variation

Engine Speed [rpm]	P_0 $\left[10^{-4}\,\frac{gr}{s}\right]$	P_1 $\left[10^{-5}\,\frac{gr}{s.N.m}\right]$	P_2 $\left[10^{-8}\,\frac{gr}{s.N^2.m^2}\right]$	P_3 $\left[10^{-10}\,\frac{gr}{s.N^3.m^3}\right]$
1000	2.8	0.47	0.11	0.14
2000	5.5	1.11	-0.33	0.15
3000	9.5	1.95	-2.62	0.57
4000	14.2	2.65	-4.15	0.95
5000	18.9	2.84	-1.01	0.77
6000	24.5	3.68	-2.02	1.53

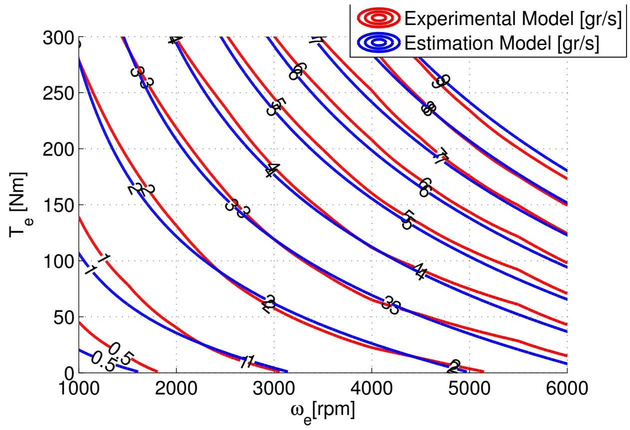

Fig. 1. Comparison of fuel consumption maps of the experimental and estimation fuel consumption models.

$$\dot{m}_f = C_5\cdot T_e(t)\cdot v(t) + C_6\cdot v(t)^2 + C_7\cdot v(t) + C_8. \qquad (3)$$

with the constants defined as

$$C_5 = \frac{\gamma(t)}{e\cdot H_L\cdot R_{wh}}, \qquad (4)$$
$$C_6 = -\frac{P_{loss}\cdot V_d}{e\cdot H_L\cdot 4\pi}\cdot\left(\frac{\gamma(t)}{R_{wh}}\right)^2, \qquad (5)$$
$$C_7 = -\frac{P_{loss}\cdot V_d}{e\cdot H_L\cdot 4\pi}\cdot\left(\frac{\gamma(t)}{R_{wh}}\right), \qquad (6)$$
$$C_8 = \dot{m}_{f,idle}, \qquad (7)$$

where, e is the average engine efficiency, H_L is the lower heating values of the fuel, P_{loss} is the average engine friction term, V_d is the displacement volume of the engine, and $\dot{m}_{f,idle}$ is the idle speed fuel consumption.

The comparison of the experimental fuel consumption and the estimation models is given in the Fig. 1. The contour plots indicate the estimation model became more accurate at overall engine operation regions.

3. OPTIMAL CONTROL FORMULATION

The main goal of the work presented in this paper is to minimize the fuel consumption along a route with varying grade.

This problem belongs to the general non-linear optimal control problem with linear control. As we do not specify the terminal time it has free terminal time but fixed initial conditions. The state dynamics are piece-wise linear and switching based on the change in road grade. The cost functional of such problem can be written as

$$J = \left[\rho^T \psi(z(t_f))\right] + \sum_{i=1}^{M} \left[\pi_i^T N_i(z(t_i))\right] + \sum_{i=1}^{M} \int_{t_{i-1}}^{t_i} \{L(z(t),u(t)) + \lambda(t)^T f_i(z(t),u(t)) - \lambda(t)^T \dot{z}(t)\}\, dt, \tag{8}$$

and,

$$f_i(z(t),u(t)) = f_{0,i}(z(t)) + f_1(z(t))u(t) \quad for \quad i = 1,2,\cdots,M \tag{9}$$

$$L(z(t),u(t)) = g_0(z(t)) + g_1(z(t))u(t), \tag{10}$$

where, z is the system states, $\psi(z(t_f))$ is the terminal boundary condition, $N_i(z(t_i))$ is the i^{th} grade change condition, M is the number of different grade regions, $L(z,u)$ is the cost function that is desired to be minimized, $f_i(z(t),u(t))$ is state equation at the i^{th} grade region, λ,ρ and π are the costate and Lagrange multipliers and t_i for $i = 1,2,\cdots,M-1$ is unspecified times of arrival to each grade change point and $t_M = t_f$ is the free terminal time.

The Hamiltonian Function is defined as:

$$H_i(z(t),u(t),\lambda(t)) = L(z(t),u(t)) + \lambda^T f_i(z(t),u(t)) \quad for \quad i = 1,2,\cdots,M \tag{11}$$

From calculus of variation theory (Bryson and Ho (1975) and Kirk (2012)) the optimal trajectories minimizing J, render $\delta J = 0$

$$\begin{aligned}\delta J = &\left[\left(\rho^T \frac{\partial \psi}{\partial t} + L + \lambda^T \dot{z}\right) dt\right]_{t=t_f} + \left[\left(\rho^T \frac{\partial \psi}{\partial z} - \lambda^T\right) dz\right]_{z=z(t_f)} \\ &+ \sum_{i=1}^{M} \left[\left(\pi_i^T \frac{\partial N_i}{\partial z} - \lambda^T(t_i^-) + \lambda^T(t_i^+)\right) dz\right]_{z=z(t_i)} \\ &+ \sum_{i=1}^{M} \left[\left(\pi_i^T \frac{\partial N_i}{\partial t} + H_i(t_i^-) - H_i(t_i^+)\right) dt\right]_{t=t_i} - L(t_0)dt_0 \\ &+ \lambda^T(t_0)\delta z(t_0) + \sum_{i=1}^{M} \int_{t_{i-1}}^{t_i} \left[\left(\frac{\partial H_i}{\partial z} + \dot{\lambda}^T\right)\delta z + \frac{\partial H_i}{\partial u}\delta u\right] dt = 0\end{aligned} \tag{12}$$

For fixed intial conditions $dt_0 = 0$ and $\delta z(t_0) = 0$, then the necessary conditions for optimality are

$$\dot{z} = f_{i+1}(z,u), \quad \begin{array}{ll} z(t_i) = z_0 & for\ i=0, \\ z(t_i^-) = z(t_i^+) & for\ i=1,2,\cdots M-1, \end{array} \tag{13}$$

$$\dot{\lambda}^T = -\frac{\partial H_i}{\partial z}, \tag{14}$$

$$\lambda^T(t_f) = \rho^T \frac{\partial \psi}{\partial z}, \tag{15}$$

$$\lambda^T(t_i^-) = \lambda^T(t_i^+) + \pi_i^T \frac{\partial N_i}{\partial z} \quad for\ i=1,2,\cdots M, \tag{16}$$

$$H_i(t_i^-) = H_i(t_i^+) - \pi_i^T \frac{\partial N_i}{\partial t_i} \quad for\ i=1,2,\cdots M. \tag{17}$$

$$\left(\rho^T \frac{\partial \psi}{\partial t} + L + \lambda^T \dot{z}\right)_{t=t_f} = 0, \tag{18}$$

$$\frac{\partial H_i}{\partial u} = 0 \quad for\ i=1,2,\cdots M, \tag{19}$$

For the systems with linear control input, the necessary condition

$$\frac{\partial H_i}{\partial u} = g_1(z(t)) + \lambda^T f_1(z(t)) = 0 \quad for\ i=1,2,\cdots M \tag{20}$$

is not dependent on u, therefore, if $g_1(z(t)) + \lambda^T f_1(z(t)) \neq 0$, the minimizer, u^*, occurs at the boundary satisfying

$$\left(g_1(z(t)) + \lambda^T f_1(z(t))\right)\delta u \geq 0 \tag{21}$$

for all feasible u, i.e.,

$$u^* = \begin{cases} u_{max} & if \quad g_1(z(t)) + \lambda^T f_1(z(t)) < 0 \\ u_{min} & if \quad g_1(z(t)) + \lambda^T f_1(z(t)) > 0 \end{cases} \tag{22}$$

On the other hand, for the case

$$\frac{\partial H_i}{\partial u} = g_1(z(t)) + \lambda^T f_1(z(t)) = 0, \tag{23}$$

the solution is stationary and all admissible u satisfy (20), then the corresponding trajectories are the singular arcs. Any motion on a singular arc satisfies

$$\frac{d}{dt}\left(\frac{\partial H_i}{\partial u}\right) = \left(\frac{\partial g_1}{\partial z} + \frac{\partial f_1}{\partial z}\right)\dot{z} + \dot{\lambda}^T f_1(z) = 0 \tag{24}$$

If (24) depends on u, we can determine u^*, otherwise, we take successive time derivatives of (24) until a direct relation to u is obtained. All the successive derivatives must satisfy

$$\frac{d^s}{dt^s}\left(\frac{\partial H}{\partial u}\right) = 0 \quad for \quad s = 1,2,\cdots. \tag{25}$$

4. ANALYTICAL SOLUTION DEVELOPMENT

In this example case, we solve a minimum fuel consumption optimization problem of a route with given (measured) grade profile using the analytical solution defined in the preceding section and compare the result with DP solution developed for the same route but for full vehicle model as described by Wollaeger et al. (2012). The initial and the terminal conditions are

$$z(0) = \begin{bmatrix} x(0) \\ v(0) \end{bmatrix} = \begin{bmatrix} 0 \\ 0 \end{bmatrix}, \quad z(t_f) = \begin{bmatrix} x(t_f) \\ v(t_f) \end{bmatrix} = \begin{bmatrix} x_{final} \\ 0 \end{bmatrix} \tag{26}$$

where, $x(t)$ is the position of the vehicle, $v(t)$ is the vehicle speed and $z(t)$ is the state vector of the system. By using (1), we can write the state dynamic equations as

$$\dot{z} = \begin{bmatrix} \dot{x} \\ \dot{v} \end{bmatrix} = f_i(z(t),u(t)) = f_{0,i}(z(t)) + f_1(z(t))u(t) \tag{27}$$

where,

$$f_{0,i}(z) = \begin{bmatrix} v \\ \frac{-C_3^* v - C_4^*(\alpha_i)}{C_1} \end{bmatrix} \quad f_1(z) = \begin{bmatrix} 0 & 0 \\ \frac{C_2}{C_1} & \frac{-1}{C_1} \end{bmatrix}, \quad u = \begin{bmatrix} T_e \\ F_{brake} \end{bmatrix}. \tag{28}$$

The cost function that we desire to minimize is the fuel consumption of the vehicle and using (3) we write it as

$$L(z(t),u(t)) = g_0(z(t)) + g_1(z(t))u(t) \tag{29}$$

where,

$$g_0(z(t)) = C_6 z_2(t)^2 + C_7 z_2(t) + C_8, \tag{30}$$

$$g_1(z(t)) = [C_5 z_2(t) \quad 0] \tag{31}$$

4.1 Solution to State Equations

The solution of the differential equations given in (27) and (28) governing the system state trajectories for $i = 1, 2, \cdots, M$ are

$$\begin{aligned} z_1(t) =& \frac{C_1}{C_3^{*2}} \left(C_2 u_1(t) - C_4^*(\alpha_i) - u_2(t) - C_3^* z_2(t_{i-1})\right) \cdot e^{\frac{-C_3}{C_1}\tau_i} \\ &+ \frac{1}{C_3}\left(C_2 u_1(t) - C_4^* - u_2(t)\right)\tau_i - \frac{C_1}{C_3^{*2}}\left(C_2 u_1(t) - C_4^*(\alpha_i)\right. \\ &\left. - u_2(t) - C_3^* z_2(0)\right) + z_1(t_{i-1}) \end{aligned} \tag{32}$$

$$\begin{aligned} z_2(t) =& \frac{-1}{C_3^*}\left(C_2 u_1(t) - C_4^*(\alpha_i) - u_2(t) - C_3^* z_2(t_{i-1})\right) \cdot e^{\frac{-C_3}{C_1}\tau_i} \\ &+ \frac{1}{C_3}\left(C_2 u_1(t) - C_4^*(\alpha_i) - u_2(t)\right) \end{aligned} \tag{33}$$

where,

$$\tau_i = t - t_{i-1} \tag{34}$$

The trajectories of $z_1(t)$ and $z_2(t)$ depends on the piece-wise constant grade, α_i, and calculated for each $i = 1, 2, \cdots, M$ with the initial condition and interior constraints given in (13) and (26).

4.2 Solution to Co-State Equations

The necessary condition derived in (14) govern the rate of change of co-state functions, $\lambda_1(t)$ and $\lambda_2(t)$. For the velocity profile optimization problem the formulations of co-state dynamics are

$$\dot{\lambda}_1(t) = \frac{-\delta H_i}{z_1} = 0 \tag{35}$$

$$\dot{\lambda}_2(t) = \frac{-\delta H_i}{z_2} = -C_5 u_1(t) - 2C_6 z_2(t) - C_7 + \frac{C_3^*}{C_1}\lambda_2(t) - \lambda_1 \tag{36}$$

We solve the differential equations defined above and determine the trajectories as

$$\lambda_1(t) = K_{1,i} \tag{37}$$

$$\begin{aligned} \lambda_2(t) =& K_{2,i} e^{\frac{C_3}{C_1}\tau_i} - \frac{C_1 C_6}{C_3^{*2}}\left(C_2 u_1(t) - C_4^* - u_2(t) - C_3^* z_2(0)\right) e^{\frac{-C_3}{C_1}\tau_i} \\ &+ \frac{2C_1 C_6}{C_3^{*2}}\left(C_2 u_1(t) - C_4^* - u_2(t)\right) + \frac{C_1}{C_3^*}\left(C_5 u_1 + C_7 K_{1,i}\right) \end{aligned} \tag{38}$$

Similar to state equations, for each $i = 1, 2, \cdots, M$, we determine the parameters $K_{1,i}$ and $K_{2,i}$ to satisfy the interior constraints given in (16). The initial conditions of λ are not defined, however, the optimal $K_{1,i}$ are problem independent and determined by solving the unconstrained optimization problem as described by Ozatay et al. (2012) such that the trajectories reach to the arc at the same time. To calculate the initial value of $K_{2,i}$, we determine the the values of $\lambda_2(t)$ and $z_2(t)$ at the closest singular arc, and solve the differential equations (33) and (38). The section 4.5 gives a detailed calculation procedure of the co-states.

4.3 Optimal Control Laws

In (21), we have determined the necessary condition of the optimal control law for the system with linear input. For the example problem, using (28) and (31) the necessary condition becomes

$$\left(C_5 z_2(t) + \frac{C_2}{C_1}\lambda_2(t)\right)\delta u_1(t) \geq 0 \tag{39}$$

$$\left(\frac{-1}{C_1}\lambda_2(t)\right)\delta u_2(t) \geq 0 \tag{40}$$

Then, u^* is determined as

$$u_1^* = \begin{cases} u_{1,max} & if \quad \left(C_5 z_2(t) + \frac{C_2}{C_1}\lambda_2(t)\right) < 0 \\ u_{1,min} & if \quad \left(C_5 z_2(t) + \frac{C_2}{C_1}\lambda_2(t)\right) > 0 \end{cases} \tag{41}$$

$$u_2^* = \begin{cases} u_{2,max} & if \quad \left(\frac{-1}{C_1}\lambda_2(t)\right) < 0 \\ u_{2,min} & if \quad \left(\frac{-1}{C_1}\lambda_2(t)\right) > 0 \end{cases} \tag{42}$$

The above minimizer is valid for the cases when the system states are not on singular arcs. We also need to determine the optimal control inputs and state trajectories on a singular arc.

4.4 Control Inputs and State Trajectories on Singular Arcs

The conditions of singularity for u_1 and u_2 are

$$\textbf{for } u_1 \quad C_5 z_2(t) + \frac{C_2}{C_1}\lambda_2(t) = 0, \quad \longrightarrow \quad \lambda_2(t) = -\frac{C_1 C_5}{C_2} z_2(t) \tag{43}$$

$$\textbf{for } u_2 \quad \frac{-1}{C_1}\lambda_2(t) = 0 \quad \longrightarrow \quad \lambda_2(t) = 0. \tag{44}$$

From (24) any motion on a singular arc must also satisfy

$$\textbf{for } u_1 \quad C_5 \dot{z}_2(t) + \frac{C_2}{C_1}\dot{\lambda}_2(t) = 0, \tag{45}$$

$$\textbf{for } u_2 \quad \dot{\lambda}_2(t) = 0. \tag{46}$$

Then, using (27), (36), (43) and (45) we determine the trajectories on the singular arc enforced by u_1 as

$$z_1(t) = \frac{-\left(C_4^*(\alpha_i)C_5 + C_2 C_7 + C_1 K_{1,i}\right)}{2\left(C_3^* C_5 + C_2 C_6\right)} t + z_1(t_{i-1}), \tag{47}$$

$$z_2(t) = \frac{-\left(C_4^*(\alpha_i)C_5 + C_2 C_7 + C_1 K_{1,i}\right)}{2\left(C_3^* C_5 + C_2 C_6\right)}, \tag{48}$$

$$\lambda_1(t) = K_{1,i}, \tag{49}$$

$$\lambda_2(t) = \frac{\left(C_1 C_4^*(\alpha_i) C_5^2 + C_1 C_2 C_7 C_5 + C_1^2 K_{1,i} C_5\right)}{2C_2\left(C_3^* C_5 + C_2 C_6\right)}, \tag{50}$$

$$u_1(t) = \frac{C_3^* z_2 + C_4^*(\alpha_i)}{C_2}, \tag{51}$$

$$u_2(t) = 0. \tag{52}$$

Similarly, inserting (27) and (36) in (44) and (46), we obtain equation of motion on the singular arc enforced by u_2 as

$$z_1(t) = \frac{-\left(C_7 + K_{1,i}\right)}{2C_6} t + z_1(t_{i-1}) \tag{53}$$

$$z_2(t) = \frac{-\left(C_7 + K_{1,i}\right)}{2C_6} \tag{54}$$

$$\lambda_1(t) = K_{1,i} \tag{55}$$

$$\lambda_2(t) = 0, \tag{56}$$

$$u_1(t) = 0, \tag{57}$$

$$u_2(t) = \frac{C_3^*\left(C_7 + K_{1,i}\right)}{2C_6} - C_4^*(\alpha_i) \tag{58}$$

Any control input on singular arcs inherently satisfy (19). Intuitively, we can also claim that the singular solutions for

u_1 and u_2 can not occur simultaneously as that implies $z_2(t) = v(t) = 0$.

4.5 Algorithm

In this section we present the procedure that is used to calculate the optimal velocity trajectory by using the solutions defined in the preceding section. Algorithm 1 initially determines the $K_{1,i} \quad for \quad i = 1, 2, \cdots, M$ from the unconstrained optimization described by Ozatay et al. (2012), then determines whether the state trajectories are governed by the singular or non-singular solutions at each grade region. To determine the singularity of the solution, the algorithm calculates the feasibility of $u_1(t)$. If $u_1(t)$ is feasible, then at that particular grade region, the optimal trajectories converge to a singular arc (as long as the grade region is long enough). Otherwise, the solution belongs to non-singular solution.

Algorithm 1 Analytic Solution Procedure

Initialize: Gear
for $i \leftarrow 1, M$ **do**
    $K_{1,i} \leftarrow$ SolutionToUnconstraintProblem(α_i)
end for
GroupNumber $\leftarrow 0$
SingularReg[GroupNumber] $\leftarrow 0$
NonSingularReg[GroupNumber] $\leftarrow 0$
boolval $\leftarrow$ **true**
for $i \leftarrow 1, M$ **do**
    if (u_1 on Sing. Arc is feasible) & (boolval) **then**
        SingularReg[GroupNumber]++
    else if (u_1 on Singular Arc is not feasible) **then**
        NonSingularReg[GroupNumber]++
        boolval $\leftarrow$ **false**
    else
        GroupNumber++
        boolval $\leftarrow$ **true**
        SingularReg[GroupNumber] $\leftarrow 0$
        NonSingularReg[GroupNumber] $\leftarrow 0$
    end if
end for

for $k \leftarrow 1$, GroupNumber **do**
    for $n \leftarrow 1$, SingularReg[GroupNumber] **do**
        Solution on Singular Arc,
    end for
    for $m \leftarrow 1$, NonSingularReg[GroupNumber] **do**
        Solution out of Singular Arc,
    end for
end for

The algorithm then group each region such that each group starts with singular solutions and ends with non-singular solutions and solves the problem separately for each group.

5. EXAMPLES WITH FICTITIOUS AND MEASURED GRADE PROFILES

This section presents the solution of the analytical solution to example problems and comparison with DP and constant speed cruise control solutions. The study by Ozatay et al. (2013a) presents the details of the DP solution. Briefly, the DP solution is developed for full vehicle model including gear shifting and torque converter models. Moreover it uses the fuel consumption model given in (2). On the other hand, the constant speed cruise control system operates at the optimal constant speed assuming level road along the route.

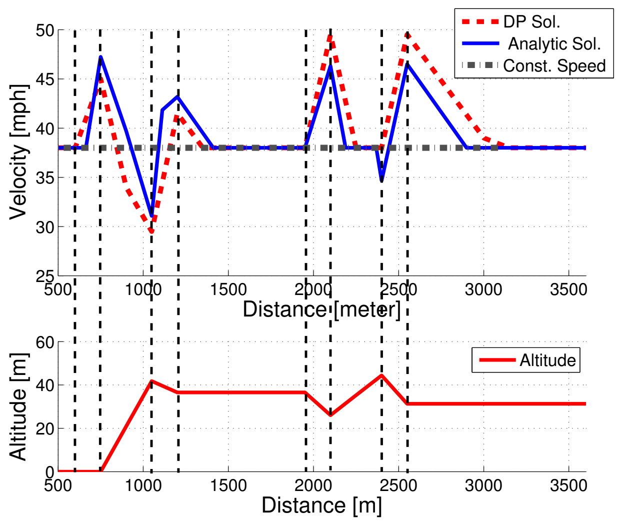

Fig. 2. The comparison of optimal speed trajectories obtained by DP and analytical solution and constant speed profile and the altitude profile of example-1

Table 2. Comparison of DP, Analytical and Constant Speed Solution for Example-1

	DP Sol	Analytical Sol.	Const. Speed
Fuel Eco. [mpg]	32.70	32.71	29.31
Improvement [%]	10.4	10.4	-
Calc. Time [sec]	16.2	0.05	0
Trip Time [min]	3.13	3.14	3.24

In the first example, we generate a fictitious road grade profile consisting a combination of positive, negative and zero slope regions as shown in the Fig. 2. In the second problem we use the measured road grade profile obtained by accurate RT3000 sensor. We also verify the accuracy of the sensor by comparing the elevation data with the information retrieved from the ArcGIS server located at Ohio Supercomputing Center (OSC). The Fig. 3 presents the elevation profile of the test route employed in example-2.

The comparison of the velocity profiles for example-1 are presented in the Fig. 2. Both trajectories propose to increase of velocity before reaching to a high positive grade region. Then at positive grade region the optimal velocity profiles start to decrease until it is recovered by the following negative grade region. At the level road region both trajectories converge back to the optimal singular solution defined in the section 4.4. On the singular arc as soon as a negative slope region is encountered the trajectories propose increase in speed with gravity force, then at the positive grade the trajectories converge back to optimal constant velocity. The numerical results given in table 2 compare the fuel economy, calculation time and trip time of the three velocity profiles. The analytical and DP solution propose 10.4% improvement in fuel economy compared to the constant cruise speed case, with out any increase in the trip time. Although, having similar results, the analytical solution overcomes the DP solution in terms of calculation time, proposing 324x times speed up.

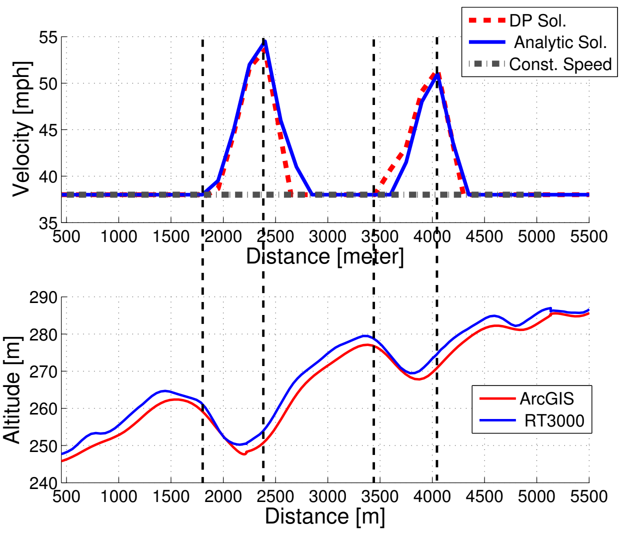

Fig. 3. The comparison of optimal speed trajectories obtained by DP and analytical solution and constant speed profile and the measured altitude of example-2

Table 3. Comparison of DP, Analytical and Constant Speed Solution for Example-2

	DP Sol	Anlaytical Sol.	Const. Speed
Fuel Eco. [mpg]	28.60	28.56	26.32
Improvement [%]	8.0	7.8	-
Calc. Time [sec]	33.6	0.06	0
Trip Time [sec]	4.75	4.76	5.00

The optimal velocity profiles to the second problem are given in the Fig. 3. Consistent to the DP solution, before reaching to the first negative grade region the analytical solution propose the speed trajectory to lie along the singular arc as the positive road grade is not high enough and the vehicle engine can supply adequate torque. When the vehicle reaches the negative grade the optimal velocity trajectories increase due to the gravitational force. Similar to the results obtained in example-1, the optimal trajectories converge back to optimal singular solution at the end of the negative grade region.

The comparison of the numerical results of each speed trajectory is reported in table 3. Again the DP and analytical solution have very close fuel economy values, and around 8% more efficient than constant speed cruise solution without any increase in the trip time. The calculation time of analytical solution is 560x times faster than the DP solution.

6. CONCLUSION

In this study, we have developed a vehicle model linearized at the optimal constant speed by assuming constant gear operation. Then we designed an accurate but yet simple fuel consumption estimation model. With the use of calculus of variation theory we designed a nonlinear optimal control problem, derived the necessary conditions and applied the results to the minimum fuel consumption optimization problem with varying road grade profile. We employed the obtained solution to generate optimal velocity profiles for two example problems and compared the results with DP solution and a constant speed profile The results have shown that the DP and analytical solution are consistent, and around $8-10\%$ more efficient than the constant cruise speed operation. Additionally, the calculation time of the analytical solution is significantly lower than DP solution. Contrary to DP , the calculation time also does not significantly change with trip distances. The results obtained in this study also proves that the analytical solution is stable, accurate and its real time implementation to on board systems is possible.

REFERENCES

Bryson, A.E. and Ho, Y.C. (1975). *Applied optimal control: optimization, estimation, and control*. Taylor & Francis.

Chang, D. and Morlok, E. (2005). Vehicle speed profiles to minimize work and fuel consumption. *Journal of Transportation Engineering*, 131(3), 173–182.

Dargay, J., Gately, D., and Sommer, M. (2007). Vehicle ownership and income growth, worldwide: 1960-2030. *The Energy Journal*, 143–170.

Guzzella, L. and Onder, C.H. (2010). *Introduction to modeling and control of internal combustion engine systems*. Springer.

Hellstrom, E., Aslund, J., and Nielsen, L. (2010). Design of an efficient algorithm for fuel-optimal look-ahead control. *Control Engineering Practice*, 18(11), 1318 – 1327.

Hellstrom, E., Ivarsson, M., Aslund, J., and Nielsen, L. (2009). Look-ahead control for heavy trucks to minimize trip time and fuel consumption. *Control Engineering Practice*, 17(2), 245 – 254.

Kirk, D.E. (2012). *Optimal control theory: an introduction*. DoverPublications. com.

Owen, N.A., Inderwildi, O.R., and King, D.A. (2010). The status of conventional world oil reserveshype or cause for concern? *Energy Policy*, 38(8), 4743 – 4749.

Ozatay, E., Onori, S., Wollaeger, J., Ozguner, U., Rizzoni, G., Filev, D., Michelini, J., and Cairano, S.D. (2013a). Cloud-based velocity profile optimization for everyday driving: a dynamic programming based solution. IEEE Transactions of Intelligent Transportation Systems, Under Review.

Ozatay, E., Ozguner, U., Filev, D., and Michelini., J. (2013b). Analytical and numerical solutions for energy minimization of on road vehicles with the existence of multiple traffic lights. In *Conference on Decision and Control*. IEEE Control Systems Society, Florence, Italy.

Ozatay, E., Ozguner, U., Onori, S., and Rizzoni, G. (2012). Analytical solution to the minimum fuel consumption optimization problem with the existence of a traffic light. In *Dynamic Systems and Control Conference 2012*, volume 1, 837–846. Fort Lauderdale, Florida, USA.

Schwarzkopf, A. and Leipnik, R. (1977). Control of highway vehicles for minimum fuel consumption over varying terrain. *Transportation Research*, 11(4), 279 – 286.

Wollaeger, J., Kumar, S., Onori, S., Filev, D., Ozguner, U., Rizzoni, G., and Di Cairano, S. (2012). Cloud-computing based velocity profile generation for minimum fuel consumption: A dynamic programming based solution. In *American Control Conference (ACC), 2012*, 2108–2113.